Computational Materials Science 53 (2012) 214–219

Contents lists available at SciVerse ScienceDirect

Computational Materials Science

journal homepage: www.elsevier.com/locate/commatsci

On the influence of the shear deformation and boundary conditions on the transverse vibration of multi-walled carbon nanotubes

Daniel Ambrosini *, Fernanda de Borbón

Structural Engineering Master Program, Engineering Faculty, National University of Cuyo, Centro Universitario, Parque Gral. San Martín, 5500 Mendoza, Argentina
National Research Council CONICET, Argentina

ARTICLE INFO

Article history:
Received 29 July 2011
Received in revised form 30 August 2011
Accepted 8 September 2011

Keywords:
Multi-walled carbon nanotubes
Vibration analysis
Continuum-beam model
Natural frequencies

ABSTRACT

The vibrational properties of multi-walled carbon nanotubes (MWCNTs) are studied, especially the influence of the shear deformation and the boundary conditions on the non-coaxial frequencies. A high order continuum beam model is proposed, which can be applied to study the transverse vibrations of MWCNTs, including those that could have initial deformations due to defects or external actions. Using the model it was found that the non-coaxial intertube frequencies are independent of the shear deformation and the boundary conditions. This result is important considering that the concentric structure of MWCNTs is a crucial geometrical characteristic and a non-coaxial vibration would affect their electronic and optical properties.

1. Introduction

The vibrational behavior of carbon nanotubes (CNTs) is very important in the design of materials for nanoelectronics, nanodevices, nanocomposites and specific applications as nanotweezers and antiferromegnetic atomic force microscopy (AFM) tips [1,2]. Moreover, often shorter CNTs are preferred to prevent undesirable kinking and buckling.

Experimental tests at nanoscale are very cumbersome and molecular simulation is computationally very expensive for large scale systems still for cluster of computers. For this reason, continuum mechanical models are an attractive alternative to study the vibrational properties of multi-walled carbon nanotubes (MWCNTs) [3].

In the frame of continuum mechanics and finite element method (FEM) there are four main alternatives: Beam model, shell model [4], spring-mass model [5] and 3D truss model [6,7]. As it was demonstrated in [8,9] it is contended that the accuracy of the shell FEM solution and a high order beam model (HBM) are comparable. Obviously, the accuracy of the FEM solution can be improved adding elements, but with a higher computational cost.

On the other hand, in the frame of beam models, the following main alternatives could be selected: (a) single-beam model [10,11] in which is assumed that all nested individual tubes of a MWCNT remain coaxial during vibration and thus can be described by a single deflection curve. Obviously, such a model cannot be used to study non-coaxial intertube vibrations of MWCNTs. (b) N-beam model in which each CNT is modeled as individual elastic beam interacting each other by the interlayer van der Waals (vdW) interaction forces. For this alternative, in most papers, Euler–Bernoulli beam model (EBM) is used [12–14] but some papers use Timoshenko beam model (TBM) [15–17] and HBM [18].

The main objective of this paper is to propose a HBM which can be applied to study the transverse vibrations of MWCNTs, including those that could have initial deformations due to defects or external actions. The model is based on the theory for thin-walled beams developed by Ambrosini et al [19] and considers shear deformations, rotatory inertia and the interlayer vdW interaction forces. The proposed model can be applied for any boundary condition. Using the model, a numerical study was carried out and it was found that the non-coaxial intertube frequencies are independent of the shear deformations and the boundary conditions.

2. Continuum model for MWCNT

A left-handed rectangular global coordinates system (x, y, z) shown in Fig. 1 is adopted. The associated displacements are designated ξ, η, and ζ. In Fig. 1, A represents the centroid and O the shear center. Obviously, for concentric MWCNTs, A and O are coincident, but in some cases the nanotubes could have initial deformations due to, e.g., defects, external actions, attached masses in CNT-based resonators, etc. In this case, the general model should be applied. When A and O are coincident, as a result of the axial

* Corresponding author at: Structural Engineering Master Program, Engineering Faculty, National University of Cuyo, Centro Universitario, Parque Gral. San Martín, 5500 Mendoza, Argentina. Tel.: +54 2627 559947; fax: +54 261 4380120.
E-mail address: dambrosini@uncu.edu.ar (D. Ambrosini).

0927-0256/$ - see front matter © 2011 Elsevier B.V. All rights reserved.
doi:10.1016/j.commatsci.2011.09.009

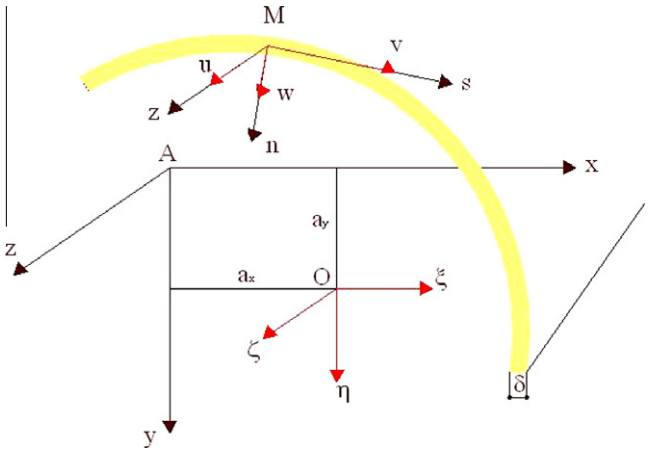

Fig. 1. Coordinate systems and associated displacements.

symmetry of nanotubes, only displacement ξ is considered in plane xy.

A single elastic beam model cannot describe the relative inter-tube vibrations for a double or multiwalled carbon nanotube. A multiple beam model is presented in this paper. In the MWCNT model, each of the nested nanotubes is described as an individual elastic beam, and the flexural deflections of all nested tubes are coupled through the vdW interaction between any two adjacent tubes. The torsional deflections remain uncoupled. Therefore, flexural and torsional vibrations of an N-wall CNT are described by the following N equations:

$$EJ_1\left(\frac{\partial^4\xi_1}{\partial z^4}-\frac{\partial^3\gamma_{m1}}{\partial z^4}\right)-\rho J_1\left(\frac{\partial^4\xi_1}{\partial z^2\partial t^2}-\frac{\partial^3\gamma_{m1}}{\partial z\partial t^2}\right)+\rho F_1\frac{\partial^2\xi_1}{\partial t^2}+a_{y1}\rho F_1\frac{\partial^2\theta_1}{\partial t^2}=c_1(\xi_2-\xi_1) \quad (1)$$

$$EJ_2\left(\frac{\partial^4\xi_2}{\partial z^4}-\frac{\partial^3\gamma_{m2}}{\partial z^4}\right)-\rho J_2\left(\frac{\partial^4\xi_2}{\partial z^2\partial t^2}-\frac{\partial^3\gamma_{m2}}{\partial z\partial t^2}\right)+\rho F_2\frac{\partial^2\xi_2}{\partial t^2}+a_{y2}\rho F_2\frac{\partial^2\theta_2}{\partial t^2}=c_2(\xi_3-\xi_2)-c_1(\xi_2-\xi_1) \quad (2)$$

$$EJ_n\left(\frac{\partial^4\xi_n}{\partial z^4}-\frac{\partial^3\gamma_{mn}}{\partial z^4}\right)-\rho J_n\left(\frac{\partial^4\xi_n}{\partial z^2\partial t^2}-\frac{\partial^3\gamma_{mn}}{\partial z\partial t^2}\right)+\rho F_n\frac{\partial^2\xi_n}{\partial t^2}+a_{yn}\rho F_n\frac{\partial^2\theta_n}{\partial t^2}=c_{n-1}(\xi_n-\xi_{n-1}) \quad (3)$$

$$EJ_{\varphi1}\frac{\partial^4\theta_1}{\partial z^4}-GJ_{d1}\frac{\partial^2\theta_1}{\partial z^2}-\rho J_{\varphi1}\frac{\partial^4\theta_1}{\partial z^2\partial t^2}+\rho F_1a_{y1}\frac{\partial^2\xi_1}{\partial t^2}+\rho J_{01}\frac{\partial^2\theta_1}{\partial t^2}=0 \quad (4)$$

$$EJ_{\varphi2}\frac{\partial^4\theta_2}{\partial z^4}-GJ_{d2}\frac{\partial^2\theta_2}{\partial z^2}-\rho J_{\varphi2}\frac{\partial^4\theta_2}{\partial z^2\partial t^2}+\rho F_2a_{y2}\frac{\partial^2\xi_2}{\partial t^2}+\rho J_{02}\frac{\partial^2\theta_2}{\partial t^2}=0 \quad (5)$$

$$EJ_{\varphi n}\frac{\partial^4\theta_n}{\partial z^4}-GJ_{dn}\frac{\partial^2\theta_n}{\partial z^2}-\rho J_{\varphi n}\frac{\partial^4\theta_n}{\partial z^2\partial t^2}+\rho F_na_{yn}\frac{\partial^2\xi_n}{\partial t^2}+\rho J_{0n}\frac{\partial^2\theta_n}{\partial t^2}=0 \quad (6)$$

In these equations the subscripts $1,2,\ldots,n$ denote the quantities of the innermost tube, its adjacent tube, and the outermost tube, respectively. E and G are the Young and shear modulus respectively, ρ denotes the mass density, J_φ is the sectorial second moment of area (warping constant), J_d is the torsion modulus, a_y is the coordinate of the shear center and J_0 is the polar moment of inertia about shear center. γ_{mi} is the mean value of the shear strain over a cross-section z = constant given by:

$$\gamma_{mi}=\frac{Q_x}{k_xF_iG} \quad (7)$$

where Q_x is the shear stress resultant on the cross section. k_x denote the Cowper's shear coefficients that could be obtained using the approximate equations given by Ebner and Billington [20]. F_i and J_i are the cross sections and the moment of inertia of the ith tube, respectively. F_i and J_i are functions of d which is the mean diameter of the nanotube and h which is the thickness of the nanotube (Fig. 2).

Several discussions have been carried about the proper value of the thickness, being 0.34 nm, the value more accepted. The mass density of the nanotube, ρ is ranged from 1.3 to 2.3 g/cm^3.

The deflections of the tubes are coupled through the vdW inter-tube interaction p. Since the inner and outer tubes are originally concentric and the vdW interaction is determined by the interlayer spacing between the tubes, the net vdW interaction pressure remains zero for each tube if they vibrate coaxially and share the same deflection curve. For a multi walled beam model, the tubes are described by individual deflections curves that may not be coincident. Therefore, for small amplitude non-coaxial linear vibration, the vdW interaction pressure at any position ξ between two tubes depends linearly of the difference of their deflection curves at that position

$$p(z)=c[\xi_2(z)-\xi_2(z)] \quad (8)$$

where c is the intertube vdW interaction coefficient. The coefficient c can be estimated as [21]:

$$c_k=\frac{320(2r_k)}{0.16a^2}\ \text{erg/cm}^2 \quad k=1,2,\ldots,n-1 \quad (9)$$

where a = 0.142 nm and r_k is the radius of the tube considered.

Using the Fourier transform, an equivalent system with eight first-order partial differential equations with eight unknowns is obtained in the frequency domain for each tube. For each nanotube, four geometric and four static unknown quantities are selected as components of the state vector v: displacement ξ,

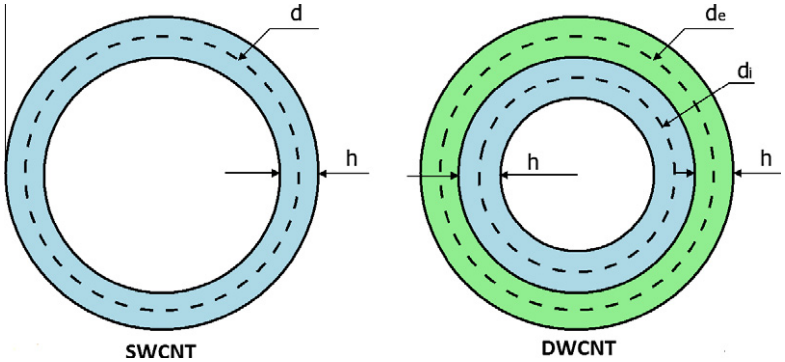

Fig. 2. Diameter and thickness definition for SWCNT and DWCNT.

Table 1
Fundamental frequency (THz). Nanotube *A*.

	DT	DE	ST	SE
Yoon et al. [17]	0.0728	0.0745	0.0731	0.0746
This paper	0.0728	0.0742	0.0731	0.0742
Difference %	0.00	0.40	0.00	0.54

Table 2
Fundamental frequency (THz). Nanotube *B*.

	DT	DE	ST	SE
Yoon et al. [17]	0.141	0.144	0.141	0.144
This paper	0.140	0.143	0.140	0.144
Difference %	0.71	0.69	0.71	0.00

bending rotation ϕ_x, normal shear stress resultant Q_x, bending moment M_y, torsional rotation θ and its spatial derivative θ', total torsional moment M_T and bimoment B:

$$v_i(z,\omega) = \{\xi, \phi_y, Q_x, M_y, \theta, \theta', M_t, B\}^T \tag{10}$$

in which, the torsional moment is given by

$$M_T = H_\varphi + H_K \tag{11}$$

with $H_K = GJ_d\ \theta'$ = Saint Venant torsion moment and H_φ is the flexural–torsional moment with respect to the shear center due to the axial stress forces which act along the tangent to the arc of the section contour.

After some mathematical operations, the final system obtained is:

$$\frac{\partial v}{\partial z} = Av \tag{12}$$

in which $A(A_{ij})$ is the system matrix given by:

$$A = \begin{bmatrix} A_{11} & A_{12} & \cdots & A_{1n} \\ A_{21} & A_{22} & \cdots & A_{2n} \\ \vdots & \vdots & \ddots & \vdots \\ A_{n1} & A_{n2} & \cdots & A_{nn} \end{bmatrix} \tag{13}$$

The A_{ii} matrix has the data of the ith nanotube. The A_{ij} matrix with $i \neq j$, has the vdW coefficient coupling the nanotubes. For the particular case of a DWCNT, the A matrix is given in Appendix A. When the nanotubes are concentric, the model can exclude the analysis of the warping constraint, reducing the system to a six first-order partial differential equations with six unknowns. In this case the sate vector is:

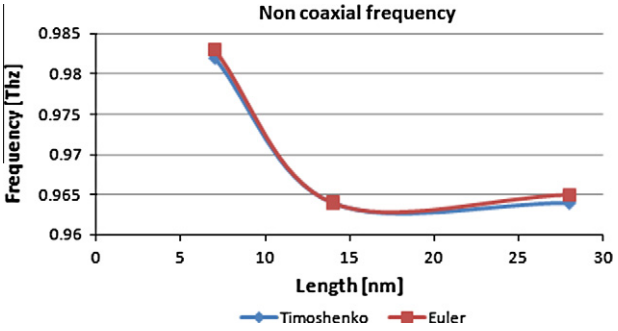

Fig. 3. Non-coaxial frequencies. DWCNT simply supported.

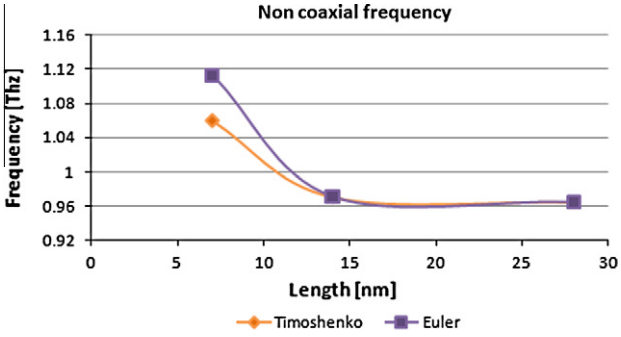

Fig. 4. Non-coaxial frequencies. DWCNT clamped–clamped.

$$v_i^*(z,\omega) = \{\xi, \phi_y, Q_x, M_y, \theta, M_t^*\}^T \tag{14}$$

where M_t^* is the torsional moment given only for the Saint Venant torsion moment. Furthermore, the coordinates of the shear center with the centroid are coincident, therefore $a_y = 0$. The new system is:

$$\frac{\partial v^*}{\partial z} = A^* v^* \tag{15}$$

For a DWCNT A^* is given in Appendix A.

The system A^* may be easily integrated using standard numerical procedures, such as the fourth-order Runge-Kutta method, the predictor – corrector algorithm or other approaches. In order to solve the two-point value problem encountered both in the determination of natural frequencies and in dynamic response calculations, the latter must be transformed to an initial value problem as shown, for example, by Ebner and Billington [20]. The procedure is normally applied in the transfer matrix method. Natural fre-

Table 3
Fundamental frequency (THz). Nanotube *A*. Simply supported.

	L = 7 nm			L = 14 nm			L = 28 nm		
	DT	DE	Diff. %	DT	DE	Diff. %	DT	DE	Diff. %
Coaxial	0.272	0.289	6.25	0.0728	0.0742	1.92	0.0185	0.0186	0.54
Non-coaxial	0.982	0.983	0.10	0.964	0.964	0.00	0.964	0.965	0.10

Table 4
Fundamental frequency (THz). Nanotube *A*. Clamped–clamped.

	L = 7 nm			L = 14 nm			L = 28 nm		
	DT	DE	Diff. %	DT	DE	Diff. %	DT	DE	Diff. %
Coaxial	0.502	0.628	20.0	0.154	0.167	7.88	0.041	0.042	1.80
Non-coaxial	1.060	1.113	4.76	0.971	0.971	0.05	0.965	0.965	0.00

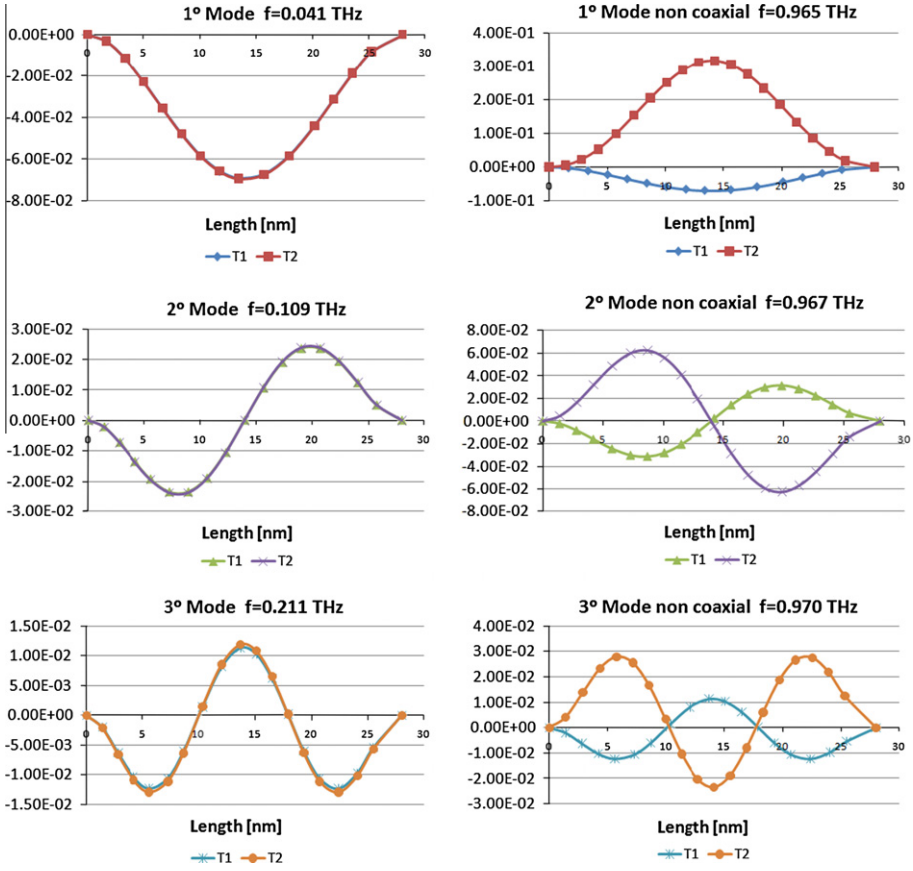

Fig. 5. Natural frequencies and modal shapes. DWCNT clamped–clamped.

Table 5
Fundamental frequency (THz). Commercial nanotube. Simply supported.

	L = 18.25 nm			L = 36.5 nm			L = 50.0 nm		
	DT	DE	Diff. %	DT	DE	Diff. %	DT	DE	Diff. %
Coaxial	0.116	0.123	5.77	0.0307	0.0312	1.66	0.0166	0.0167	0.90
Non-coaxial	1.386	1.409	1.63	1.386	1.401	1.07	1.393	1.402	0.64

Table 6
Fundamental frequency (THz). Commercial nanotube. Clamped–clamped.

	L = 18.25 nm			L = 36.5 nm			L = 50.0 nm		
	DT	DE	Diff. %	DT	DE	Diff. %	DT	DE	Diff. %
Coaxial	0.218	0.278	21.58	0.066	0.071	7.41	0.036	0.038	4.73
Non-coaxial	1.424	1.427	0.21	1.392	1.411	1.35	1.387	1.406	1.35

quencies are determined by means of the well-known Thomson's method.

3. Numerical results and discussion

Afterward, the coaxial and non-coaxial frequencies are obtained for nanotubes of different aspect ratios. The influence of shear deformation and boundary conditions is studied.

3.1. Model validation

In order to validate the beam model and the methodology proposed, numerical examples are reproduced from [17]. Four beam models are used: double Timoshenko (DT), double Euler (DE), single Timoshenko (ST) and single Euler (SE) beam.

The nanotubes in consideration have the following mechanical and geometric properties:

Nanotube A	Nanotube B
d_i = 0.7 nm	d_i = 7 nm
d_e = 1.4 nm	d_e = 7.7 nm
E = 1 TPa; G = 0.4 TPa	
v = 0.25; h = 0.35 nm	
k_x = 0.8; ρ = 2.3 g/cm^3	

The DWCNTs are considered simply supported. A vdW interaction coefficient $c = 200(2r)/0.16a^2$ is considered. The aspect ratio is

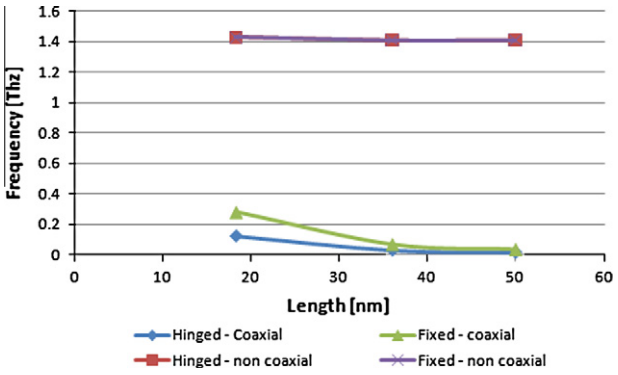

Fig. 6. Fundamental frequencies. Commercial DWCNT.

$L/d_e = 10$. The obtained results for the fundamental frequency are presented in Tables 1 and 2.

For both DWCNTs, the results obtained whit the proposed model are in excellent agreement with those of referenced paper [17].

3.2. Coaxial and non-coaxial frequencies of nanotube A

In order to investigate the vibration characteristics of different aspect ratio nanotubes (5, 10 and 20), numerical examples are carried out with the double Timoshenko (DT) and double Euler (DE) beam models. The support conditions considered are simply supported and clamped–clamped. First, the nanotube *A* corresponding to Section 3.1 is studied. The results are presented in Tables 3 and 4.

The first coaxial frequency obtained with the Timoshenko beam model is lower than the frequency of the Euler beam model for the two boundary conditions. The difference in the frequencies between the two models is 6.23% for simply supported and 20.0% for clamped, in shorter nanotubes, for the coaxial frequency. This difference diminishes in nanotubes with larger aspect ratios. These facts are consistent with the beam theories.

The first non-coaxial frequency is essentially the same for the simply supported nanotube analyzed with either the Euler or Timoshenko beam models considering different aspect ratios, indicating that the shear deformation has not influence on the non-coaxial frequency (Fig. 3).

For the clamped–clamped nanotubes, the first non-coaxial frequencies are slightly different. The 7 nm length nanotube has a higher frequency but with the increase of length, the frequencies tend to be similar (Fig. 4). Finally, for the sake of illustration, the first three frequencies and modal shapes for a clamped–clamped DWCNT of 28 nm length is showed in Fig. 5.

3.3. Coaxial and non-coaxial frequencies of commercial nanotubes

Next, a double-walled nanotube of commercial diameters is studied. The internal and external diameters are $d_i = 2.95$ and $d_e = 3.65$ nm. The vdW coefficient is considered as $c = 320(2r)/0.16a^2$. The results are presented in Tables 5 and 6 and Fig. 6.

Similar conclusions are obtained with this example. Meanwhile the first coaxial frequency changes with the increase of length of the nanotube, the non-coaxial frequency remains practically invariable for all the aspect ratios.

Analyzing the two examples, we can conclude that the non-coaxial frequency seems not to be dependent of the boundary condition of the nanotube.

In what concerns to shear deformations, the difference between the first non-coaxial frequencies obtained with the two simply supported beam models is close 0.1% for Section 3.2, excluding the shorter clamped–clamped nanotube. For the Section 3.3, the discrepancy in the non-coaxial frequencies is more important but always considerably inferior to the changes experimented for the coaxial frequency. Therefore, it can be assumed that the non-coaxial frequencies are insensitive to shear deformations.

4. Conclusions

A theoretical approach based on a HBM is proposed to study the transverse vibrations of MWCNTs, including those that could have initial deformations. The model is applicable to arbitrary boundary conditions. It was numerically validated against other results from the literature and the numerical results are in good agreement with those of referenced work.

A numerical study was carried out to study the coaxial and non-coaxial natural frequencies for DWCNTs of different aspect ratios and different boundary conditions. In what concerns to shear deformations, the difference between the first non-coaxial frequencies obtained for the two boundary conditions analyzed is small, excluding the shorter clamped–clamped nanotube. In this case, the discrepancy in the non-coaxial frequencies is more important but always considerably inferior to the changes experimented for the coaxial frequency. Therefore, it can be assumed that the non-coaxial frequencies are insensitive to shear deformations. Moreover, analyzing the numerical examples, we can conclude that the non-coaxial frequency seems not to be dependent of the boundary condition of the nanotube. These results are important taking into account that the concentric structure is the geometrical characteristic of DWCNTs, such a non-coaxial vibration would crucially affect their electronic and optical properties.

Finally, it must be emphasized that, although only concentric DWCNTs examples are presented, the proposed model allows the consideration of MWCNTs with initial deformations.

Acknowledgements

The financial support of the CONICET and the Universidad Nacional de Cuyo is gratefully acknowledged. Special acknowledgements are extended to one of the reviewers of the first version of the paper, since his useful suggestions led to improvements of the work.

Appendix A

System matrix for DWCNT. General model.

$$A = \begin{bmatrix}
0 & 1 & \frac{1}{k_x F_1 G} & 0 & 0 & 0 & 0 & 0 & 0 & 0 & 0 & 0 & 0 & 0 & 0 & 0 \\
0 & 0 & 0 & \frac{1}{EJ_1} & 0 & 0 & 0 & 0 & 0 & 0 & 0 & 0 & 0 & 0 & 0 & 0 \\
-\rho F_1 \omega^2 + c_1 & 1 & 0 & 0 & -\rho F_1 a_y \omega^2 & 0 & 0 & 0 & -c_1 & 0 & 0 & 0 & 0 & 0 & 0 & 0 \\
0 & -\rho J_1 \omega^2 & 0 & 0 & 0 & 0 & 0 & 0 & 0 & 0 & 0 & 0 & 0 & 0 & 0 & 0 \\
0 & 0 & 0 & 0 & 0 & 1 & 0 & 0 & 0 & 0 & 0 & 0 & 0 & 0 & 0 & 0 \\
0 & 0 & 0 & 0 & 0 & 0 & 0 & -\frac{1}{EJ\varphi} & 0 & 0 & 0 & 0 & 0 & 0 & 0 & 0 \\
-\rho F_1 a_y \omega^2 & 0 & 0 & 0 & -\rho J_{01} \omega^2 & 0 & 0 & 0 & 0 & 0 & 0 & 0 & 0 & 0 & 0 & 0 \\
0 & 0 & 0 & 0 & 0 & B\theta' & 1 & 0 & 0 & 0 & 0 & 0 & 0 & 0 & 0 & 0 \\
0 & 0 & 0 & 0 & 0 & 0 & 0 & 0 & 0 & 1 & \frac{1}{k_x F_2 G} & 0 & 0 & 0 & 0 & 0 \\
0 & 0 & 0 & 0 & 0 & 0 & 0 & 0 & 0 & 0 & 0 & \frac{1}{EJ_2} & 0 & 0 & 0 & 0 \\
-c_1 & 0 & 0 & 0 & 0 & 0 & 0 & 0 & -\rho F_2 \omega^2 + c & 1 & 0 & 0 & -\rho F_2 a_y \omega^2 & 0 & 0 & 0 \\
0 & 0 & 0 & 0 & 0 & 0 & 0 & 0 & 0 & -\rho J_2 \omega^2 & 0 & 0 & 0 & 0 & 0 & 0 \\
0 & 0 & 0 & 0 & 0 & 0 & 0 & 0 & 0 & 0 & 0 & 0 & 0 & 1 & 0 & 0 \\
0 & 0 & 0 & 0 & 0 & 0 & 0 & 0 & 0 & 0 & 0 & 0 & 0 & 1 & 0 & -\frac{1}{EJ\varphi} \\
0 & 0 & 0 & 0 & 0 & 0 & 0 & 0 & -\rho F_2 a_y \omega^2 & 0 & 0 & 0 & -\rho J_{02} \omega^2 & 0 & 0 & 0 \\
0 & 0 & 0 & 0 & 0 & 0 & 0 & 0 & 0 & 0 & 0 & 0 & 0 & B\theta' & 1 & 0
\end{bmatrix}$$

System matrix for DWCNT. Concentric DWCNT model.

$$A = \begin{bmatrix}
0 & 1 & \frac{1}{kF_1 G} & 0 & 0 & 0 & 0 & 0 & 0 & 0 & 0 & 0 \\
0 & 0 & 0 & \frac{1}{EJ_1} & 0 & 0 & 0 & 0 & 0 & 0 & 0 & 0 \\
-\rho F_1 \omega^2 + c_1 & 0 & 0 & 0 & 0 & 0 & -c_1 & 0 & 0 & 0 & 0 & 0 \\
0 & -\rho J_1 \omega^2 & -1 & 0 & 0 & 0 & 0 & 0 & 0 & 0 & 0 & 0 \\
0 & 0 & 0 & 0 & 0 & \frac{1}{GJ_{d1}} & 0 & 0 & 0 & 0 & 0 & 0 \\
0 & 0 & 0 & 0 & -\rho J_{01} \omega^2 & 0 & 0 & 0 & 0 & 0 & 0 & 0 \\
0 & 0 & 0 & 0 & 0 & 0 & 0 & 1 & \frac{1}{kF_2 G} & 0 & 0 & 0 \\
0 & 0 & 0 & 0 & 0 & 0 & 0 & 0 & 0 & \frac{1}{EJ_2} & 0 & 0 \\
-c_1 & 0 & 0 & 0 & 0 & 0 & -\rho F_2 \omega^2 + c_1 & 0 & 0 & 0 & 0 & 0 \\
0 & 0 & 0 & 0 & 0 & 0 & 0 & -\rho J_2 \omega^2 & -1 & 0 & 0 & 0 \\
0 & 0 & 0 & 0 & 0 & 0 & 0 & 0 & 0 & 0 & 0 & \frac{1}{GJ_{d2}} \\
0 & 0 & 0 & 0 & 0 & 0 & 0 & 0 & 0 & 0 & -\rho J_{02} \omega^2 & 0
\end{bmatrix}$$

References

[1] D. Nakabayashi, A.L.D. Moreau, V.R. Coluci, D.S. Galvão, M.A. Cotta, D. Ugarte, Nano Lett. 8 (3) (2008) 842–847.
[2] T. Natsuki, Q.Q. Ni, M. Endo, Carbon 49 (2011) 2532–2537.
[3] V.M. Harik, Comput. Mater. Sci. 24 (2002) 328–342.
[4] M. Mitra, S. Gopalakrishnan, Comput. Mater. Sci. 45 (2009) 411–418.
[5] S.K. Georgantzinos, N.K. Anifantis, Comput. Mater. Sci. 47 (2009) 168–177.
[6] U. Lee, Ch Lee, J. Sound Vib. 319 (2009) 993–1002.
[7] M. Mir, A. Hosseini, G.H. Majzoobi, Comput. Mater. Sci. 43 (2008) 540–548.
[8] D. Ambrosini, Thin Walled Struct. 47 (6–7) (2009) 629–636.
[9] D. Ambrosini, Eng. Struct. 32 (5) (2010) 1324–1332.
[10] E.W. Wong, P.E. Sheehan, C.M. Lieber, Science 277 (5334) (1997) 1971–1975.
[11] M.M.J. Treacy, T.W. Ebbesen, J.M. Gibson, Nature 381 (1996) 678–680.
[12] S. Adali, Nano Lett. 9 (5) (2009) 1737–1741.
[13] K.Y. Xu, X.N. Guo, C.Q. Ru, J. Appl. Phys. 99 (2006). 064303-7.
[14] T. Natsuki, Q. Ni, M. Endo, Carbon 46 (2008) 1570–1573.
[15] Q. Wang, V.K. Varadan, Int. J. Solids Struct. 43 (2) (2006) 254–265.
[16] J. Yoon, C.Q. Ru, A. Mioduchowski, Compos. Part B: Eng. 35 (2004) 87–93.
[17] J. Yoon, C.Q. Ru, A. Mioduchowski, J. Appl. Mech. ASME 71 (2004) 1–8.
[18] M. Aydogdu, Int. J. Mech. Sci. 50 (2008) 837–844.
[19] D. Ambrosini, J.D. Riera, R.F. Danesi, Eng. Struct. 22 (2000) 890–900.
[20] A. Ebner, D. Billington, J. Struct. Div. ASCE 94 (1968) 737–760.
[21] R. Saito, R. Matsuo, T. Kimura, G. Dresselhaus, M. Dresselhaus, Chem. Phys. Lett. 348 (3–4) (2001) 187–193.